scientific reports

Check for updates

OPEN

MRI features of breast cancer immunophenotypes with a focus on luminal estrogen receptor low positive invasive carcinomas

Carla Chizuru Tajima[1,2]✉, Fernanda Pini Sapata Gonçalves Arruda[1], Victor Chequer Mineli[1], Julianna Moura Ferreira[1], Barbara Beltrame Bettim[3], Cynthia Aparecida Bueno de Toledo Osório[4], Marina Sonagli[5] & Almir Galvão Vieira Bitencourt[6]

To compare the magnetic resonance imaging (MRI) features of different immunophenotypes of breast carcinoma of no special type (NST), with special attention to estrogen receptor (ER)-low-positive breast cancer. This retrospective, single-centre, Institutional Review Board (IRB)-approved study included 398 patients with invasive breast carcinoma. Breast carcinomas were classified as ER-low-positive when there was ER staining in 1–10% of tumour cells. Pretreatment MRI was reviewed to assess the tumour imaging features according to the 5th edition of the Breast Imaging Reporting and Data System (BI-RADS) lexicon. Of the 398 cases, 50 (12.6%) were luminal A, 191 (48.0%) were luminal B, 26 (6.5%) were luminal ER-low positive, 64 (16.1%) were HER2-overexpressing, and 67 (16.8%) were triple negative. Correlation analysis between MRI features and tumour immunophenotype showed statistically significant differences in mass shape, margins, internal enhancement and the delayed phase of the kinetic curve. An oval or round shape and rim enhancement were most frequently observed in triple-negative and luminal ER-low-positive tumours. Spiculated margins were most common in luminal A and luminal B tumours. A persistent kinetic curve was more frequent in luminal A tumours, while a washout curve was more common in the triple-negative, HER2-overexpressing and luminal ER-low-positive immunophenotypes. Multinomial regression analysis showed that luminal ER-low-positive tumours had similar results to triple-negative tumours for almost all variables. Luminal ER-low-positive tumours present with similar MRI findings to triple-negative tumours, which suggests that MRI can play a fundamental role in adequate radiopathological correlation and therapeutic planning in these patients.

Keywords Breast cancer, Estrogen receptors, Magnetic resonance imaging, Triple-negative breast neoplasms

Abbreviations

MRI	Magnetic resonance imaging
ER	Estrogen receptor
IRB	Institutional Review Board
BI-RADS	Breast Imaging Reporting and Data System
IHC	Immunohistochemical
HR	Hormone receptor
PgR	Progesterone receptor
ASCO	American Society of Clinical Oncology
CAP	College of American Pathologists
NST	No special type

[1]Imaging Department, Graduate Program of A.C.Camargo Cancer Center, São Paulo, SP, Brazil. [2]Imaging Department, A Beneficência Portuguesa de São Paulo, São Paulo, Brazil. [3]Department of Epidemiology and Statistics, A.C. Camargo Cancer Center, São Paulo, Brazil. [4]Department of Pathology, A.C. Camargo Cancer Center, São Paulo, Brazil. [5]Department of Breast Surgery, A.C. Camargo Cancer Center, São Paulo, Brazil. [6]Department of Imaging, A.C. Camargo Cancer Center, São Paulo, Brazil. ✉email: carlatajima@gmail.com

DCIS	Ductal carcinoma in situ
DISH	Dual in situ hybridization
FISH	Fluorescence in situ hybridization

Breast cancer is a heterogeneous disease. Currently, treatment planning is based not only on anatomic staging but also, and perhaps more importantly, on prognostic biomarkers[1]. Immunohistochemical (IHC) staining for hormone receptors (HRs) and HER2 allows breast cancers to be classified into different immunophenotypes and has great practical importance for treatment. The most common immunophenotype of breast cancer is the luminal phenotype, which is characterized by positive expression of HRs and usually benefits from endocrine therapy. However, there is great heterogeneity even within luminal tumours, which can be classified as luminal A, luminal B or luminal HER2 based on the expression of markers other than oestrogen receptor (ER) and progesterone receptor (PgR), such as Ki-67 and HER2, or based on recurrence risk scores[2].

The American Society of Clinical Oncology/College of American Pathologists (ASCO/CAP) guidelines recommend that ER be considered positive if 1% or more of tumour cells have nuclear staining of any intensity[3]. However, cases with ER staining in 1–10% of tumour cells should be reported as ER-low positive, since these tumours are biologically heterogeneous and often have gene expression profiles similar to ER-negative carcinomas[3–5]. There are limited data on the overall benefit of endocrine therapy for patients with these results, and many experts do not recommend it if fewer than 10% of cells express ER[6]. The pathologic and imaging features of luminal ER-low-positive breast carcinomas are not yet well described in the literature. Nevertheless, in clinical practice and some clinical trials, luminal ER-low-positive cancers have been classified and treated as triple-negative breast cancers[7–9].

Magnetic resonance imaging (MRI) is the most sensitive imaging modality for detecting breast cancer and assessing the extent of the disease[10,11]. Prior studies have shown that MRI features have a strong correlation with molecular subtypes in breast cancer[12–17]. The aim of this study was to compare the MRI features of different immunophenotypes of breast carcinoma of no special type (NST), with special attention to ER-low-positive breast cancer.

Material and methods

This retrospective, single-centre, Institutional Review Board (IRB)-approved study assessed 700 consecutive patients who were diagnosed with breast cancer and underwent pretreatment breast MRI between January 2019 and December 2020. Patients with ductal carcinoma in situ (DCIS) or special types of invasive breast carcinomas were excluded, as were those who did not have complete histological or immunohistochemical information, those whose MR images were not available for analysis, and those who were not treated in the institution (n = 302 excluded in total). Thus, 398 patients with NST invasive breast carcinomas were included (Fig. 1); these patients had a mean age of 50.1 ± 12.5 years (range 18–86 years).

Pathological evaluation

All pretreatment biopsies were reviewed by the institution's pathology department. As recommended, ER expression was considered positive if 1% or more of tumour cells had nuclear staining of any intensity. Breast carcinomas were classified as ER-low-positive when there was ER staining in 1–10% of tumour cells[3]. HER2 expression was considered positive if there was HER2 protein overexpression (grade 3+) on IHC or HER2 protein expression of grade 2+ on IHC with HER2 gene amplification detected by fluorescence in situ hybridization (FISH) or dual in situ hybridization (DISH)[18]. Immunohistochemical data were used to classify breast carcinomas into five immunophenotypes:

1. Luminal A (ER-positive >10%, HER2-negative, Ki67 < 15%, and PgR ≥ 20%);
2. Luminal B (ER-positive >10%, HER2-negative, and Ki67 ≥ 15% or PgR < 20%);

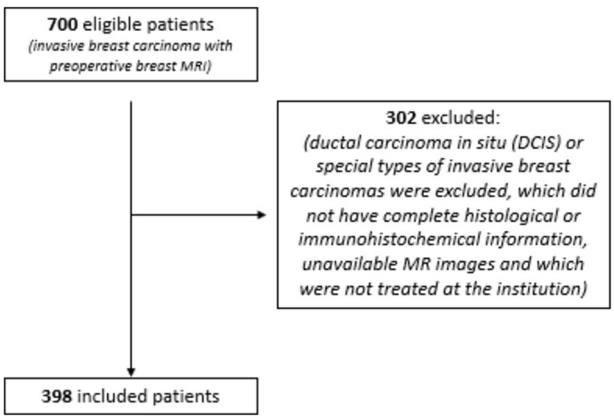

Figure 1. Flowchart of inclusion and exclusion criteria for the study.

3. Luminal ER-low positive (ER-positive 1-10%, and HER2-negative);
4. HER2 (HER2-overexpressed, ER-negative or positive);
5. Triple negative (ER-negative and HER2-negative).

MRI protocol

MRI studies were conducted with a high-field system (1.5-Tesla Achieva, Philips Healthcare, Best, Netherlands) with a dedicated 8-channel breast coil. Images were obtained before and after administration of the paramagnetic contrast agent gadopentetate dimeglumine (Gd-DTPA), at the dose of 0.1 mmol/kg body weight, with an infusion rate of 3 ml/s, followed by a saline flush. Prior to administration of Gd-DTPA, three-dimensional (3D) T1 gradient-echo imaging was acquired in the axial plane (repetition time (TR)/echo time (TE), 627/8.0 ms; 3 mm-thick slices; 280 × 399 matrix; field of view (FOV), 250 mm). A fat-saturated short-tau inversion recovery (STIR) sequence was also used to image each breast in the sagittal plane (TR/TE, 5127/80 ms; 3 mm-thick slices; 220 × 208 matrix; FOV, 220 mm). Furthermore, five 3D T1 gradient-echo phases in the axial plane were obtained by using fat suppression for dynamic examination (TR/TE, 5.1/2.5 ms; 1 mm-thick slices; 352 × 429 matrix; FOV, 300 mm). The dynamic MRI study of the breasts consisted of one pre-contrast phase, where images are acquired before contrast administration, and four post-contrast phases, with images acquired sequentially. The first post-contrast sequence started 20 s after contrast injection, followed by subsequent sequences with a temporal resolution of 60–90 s (total time: 240–360 s). The first post-contrast sequence was used for early phase enhancement analysis. Post-contrast images were subtracted from pre-contrast images to provide a better view of the highlighted areas. The last sequence consisted of a sagittal T1-weighted, 3D gradient-echo pulse sequence with fat signal suppression (TR/TE, 5.5/2.9 ms; 1 mm-thick slices; 368 × 364 matrix; FOV, 220 mm).

Pretreatment MRI was reviewed to assess the tumour imaging features according to the 5th edition of the Breast Imaging Reporting and Data System (BI-RADS®) lexicon, which included lesion type (mass and non-mass enhancement [NME]), mass shape (oval, round, or irregular), mass margins (circumscribed, irregular, or spiculated), mass internal enhancement (homogeneous, heterogeneous, or rim), mass kinetic curve—initial phase (slow, medium, or fast), mass kinetic curve—delayed phase (persistent, plateau, or washout), and NME distribution (focal, linear, segmental, regional, multiple regions, or diffuse)[19].

Statistical analysis

Statistical analyses were performed by using SPSS for Windows, version 28.0 (SPSS Inc., Chicago, IL, USA), and R software, version 4.1.3 (R Foundation for Statistical Computing, Vienna, Austria). The Pearson chi-square test with Yates's correction or Fisher's exact test was used to compare categorical variables. A multinomial regression analysis was performed to explore each imaging feature with a P value < 0.10 in the prior analyses, using the tumour immunophenotype (luminal A, luminal B, luminal ER-low-positive, and HER2) as the dependent variable. The triple-negative immunophenotype was considered the reference category for this analysis, and the results are presented as odds ratios (ORs) and 95% confidence intervals (95% CIs). The significance level was fixed at 5% for all tests; that is, p values less than 0.05 were considered to represent statistically significant results. A multiple correspondence analysis (MCA) was also performed to provide a graphical representation of the structure of correlations between MRI features and tumour immunophenotypes.

Informed consent

The need for written informed consent was waived by the Institutional Review Board.

Ethical approval

Approval was obtained from the Institutional Review Board (n. 5.430.035).

Statistics and biometry

One of the authors has significant statistical expertise.

Results

Of the 398 included cases, 50 (12.6%) were luminal A, 191 (48.0%) were luminal B, 26 (6.5%) were luminal ER-low-positive, 64 (16.1%) were HER2 (38 ER-positive and 26 ER-negative), and 67 (16.8%) were triple-negative. On MRI, 295 tumours (74.1%) presented as a mass, 53 (13.3%) presented as NME, and 50 (12.6%) presented as both a mass and NME. The complete histological and MRI data are described in Table 1.

The correlation between MRI features and tumour immunophenotype revealed significant associations with mass shape, margins, internal enhancement and delayed phase of the kinetic curve (Table 2). Oval or round shape and rim enhancement were most frequently observed in triple-negative and luminal ER-low-positive tumours (Fig. 2). Spiculated margins were most frequent in luminal A and luminal B tumours (Fig. 3). A persistent kinetic curve was more frequent in luminal A tumours, while a washout curve was more common in triple-negative, HER2-overexpressing and luminal ER-low-positive immunophenotypes (Fig. 4).

Multinomial regression analysis showed that luminal A and luminal B tumours had statistically significant differences in most variables in comparison to triple-negative tumours. On the other hand, luminal ER-low tumours had similar results to triple-negative tumours for almost all variables. HER2-overexpressing tumours showed differences in lesion type, mass shape and margins, but similar results concerning internal enhancement and kinetic curves (Table 3).

In the MCA (Fig. 5), we observed three main groups related to the imaging phenotype: in the first group, luminal A tumours were associated with spiculated margins, homogenous internal enhancement and a persistent

Variables	N (%)
MRI features	
Lesion type (n = 398)	
Mass	345 (86.7)
Non-mass enhancement (NME)	103 (25.9)
Lesion presentation (n = 398)	
Unifocal mass	217 (54.5)
Multifocal mass/NME	181 (45.5)
Mass—shape (n = 345)	
Oval/round	124 (35.9)
Irregular	221 (64.1)
Mass—margins (n = 345)	
Circumscribed	22 (6.4)
Irregular	215 (62.3)
Spiculated	108 (31.3)
Mass—internal enhancement (n = 345)	
Homogeneous	31 (9.0)
Heterogeneous	270 (78.3)
Rim enhancement	44 (12.8)
Mass—kinetic curve—initial phase (n = 345)	
Slow/medium	50 (14.5)
Fast	295 (85.5)
Mass—kinetic curve—delayed phase (n = 345)	
Persistent (type I)	84 (24.3)
Plateau	114 (33.0)
Washout	147 (42.6)
NME—distribution (n = 103)	
Focal	27 (26.2)
Linear	16 (15.5)
Segmental	46 (44.7)
Regional	9 (8.7)
Diffuse	4 (3.9)
Multiple regions	1 (1.0)
Histology/Immunohistochemistry	
Tumour grade (n = 386)	
I	62 (16.1)
II	165 (42.7)
III	159 (41.2)
Nuclear grade (n = 397)	
1	18 (4.5)
2	133 (33.5)
3	246 (62.0)
ER expression (n = 398)	
Negative	101 (25.4)
Positive	297 (74.6)
PgR expression (n = 398)	
Negative	122 (30.7)
Positive	276 (69.3)
HER2 expression (n = 398)	
Negative	324 (83.9)
Positive	64 (16.1)
Ki-67 expression (n = 398)	
< 15%	63 (15.8)
≥ 15%	325 (84.2)
Immunophenotype (n = 398)	
Luminal A	50 (12.6)
Luminal B	191 (48.0)
Continued	

Variables	N (%)
Luminal ER-low-positive	26 (6.5)
HER2	64 (16.1)
Triple-negative	67 (16.8)

Table 1. MRI features and histology/immunohistochemistry data of the included NST invasive breast carcinomas (n = 398).

Variables	Luminal A	Luminal B	Luminal ER Low	HER2	TN	*p*
Lesion type						
Mass	42 (82.4)	164 (85.9)	25 (96.2)	52 (92.5)	62 (92.5)	0.19
NME	10 (20.0)	54 (28.3)	7 (7.7)	22 (34.4)	15 (22.4)	0.06
Lesion presentation						
Unifocal mass	30 (60.0)	95 (49.7)	18 (69.2)	30 (46.9)	44 (65.7)	**0.05**
Multifocal mass/NME	20 (40.0)	96 (50.3)	8 (30.8)	34 (53.1)	23 (34.3)	
Mass—shape						
Oval/round	11 (26.2)	53 (32.3)	13 (52.0)	14 (26.9)	33 (53.2)	**< 0.01**
Irregular	31 (73.8)	111 (67.7)	12 (48.0)	38 (73.1)	29 (46.8)	
Mass—margins						
Circumscribed	5 (11.9)	7 (4.3)	2 (8.0)	3 (5.8)	5 (8.1)	**< 0.01**
Irregular	16 (38.1)	93 (56.7)	19 (76.0)	35 (67.3)	52 (83.9)	
Spiculated	21 (50.0)	64 (39.0)	4 (16.0)	14 (26.9)	5 (8.1)	
Mass—enhancement						
Homogeneous	8 (19.0)	17 (10.4)	2 (8.0)	2 (3.8)	2 (3.2)	**< 0.01**
Heterogeneous	32 (76.2)	131 (79.9)	16 (64.0)	47 (90.4)	44 (71.0)	
Rim	2 (4.8)	16 (9.8)	7 (28.0)	3 (5.8)	16 (25.8)	
Mass—early kinetic curve						
Slow/medium	7 (16.7)	32 (19.5)	2 (8.0)	3 (5.8)	6 (9.7)	0.07
Fast	35 (83.3)	132 (80.5)	23 (92.0)	49 (94.2)	56 (90.3)	
Mass—late kinetic curve						
Persistent (type I)	18 (42.9)	43 (26.2)	4 (16.0)	8 (17.3)	10 (16.1)	**< 0.01**
Plateau (type II)	19 (45.2)	53 (32.3)	11 (44.0)	18 (34.6)	13 (21.0)	
Washout (type III)	5 (11.9)	68 (41.5)	10 (40.0)	25 (48.1)	39 (62.9)	

Table 2. Analysis of MRI features associated with the immunophenotypes of NST invasive breast carcinomas. Significant values are in bold.

kinetic curve in the delayed phase; the second group was composed of luminal B and HER2-overexpressing tumours, which were mainly associated with irregular shape and margins, heterogeneous internal enhancement and a plateau or washout kinetic curve in the delayed phase; and the third group included triple-negative and luminal ER-low-positive tumours, which were mainly associated with oval or round shape, circumscribed margins, rim enhancement, a washout kinetic curve in the delayed phase and multifocal masses or NME.

Discussion

Our results show that luminal ER-low-positive tumours have similar imaging characteristics to triple-negative breast cancer, including similar lesion presentation and mass features (shape, margins, enhancement and late kinetic curve). A round or oval unifocal mass with circumscribed margins, rim enhancement and washout kinetic curve was most frequently observed in luminal ER-low-positive and triple-negative tumours in our sample.

Similar to our findings, many authors have demonstrated that triple-negative breast cancer is usually associated with a round or oval mass with circumscribed margins, rim enhancement and a washout kinetic curve[17,20–24]. On the other hand, luminal A carcinomas most commonly present as irregularly shaped unifocal masses with spiculated margins[14,17]. Luminal B carcinomas are mostly associated with heterogeneous internal enhancement[15]. Multicentric and/or multifocal disease are more commonly found in luminal B and HER2-overexpressing carcinomas[25,26]. The presence of NME, which is usually related to associated DCIS on pathology, is more frequent in the HER2-overexpressing subtype[14,27].

To our knowledge, this is the first paper reporting the MRI features of luminal ER-low-positive invasive breast carcinomas. Although luminal patients with low positive ER represent a relatively small subgroup of breast cancer patients, with an estimated prevalence of 2–7%, these tumors have different clinicopathological characteristics from other luminal tumors, such as higher histological grade, higher rates of basal-like molecular subtype on

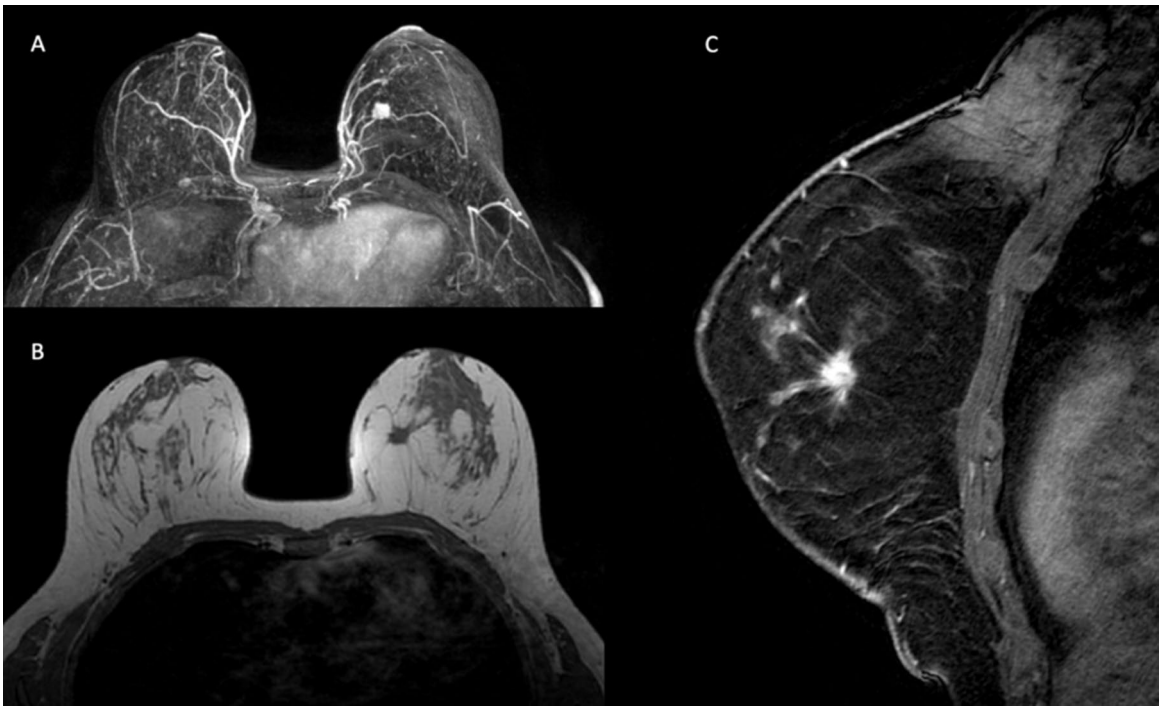

Figure 2. Irregular unifocal mass with spiculated margins in the left breast. IHC: Luminal A (ER 90%, PgR 90%, HER2 -, Ki67 10%).

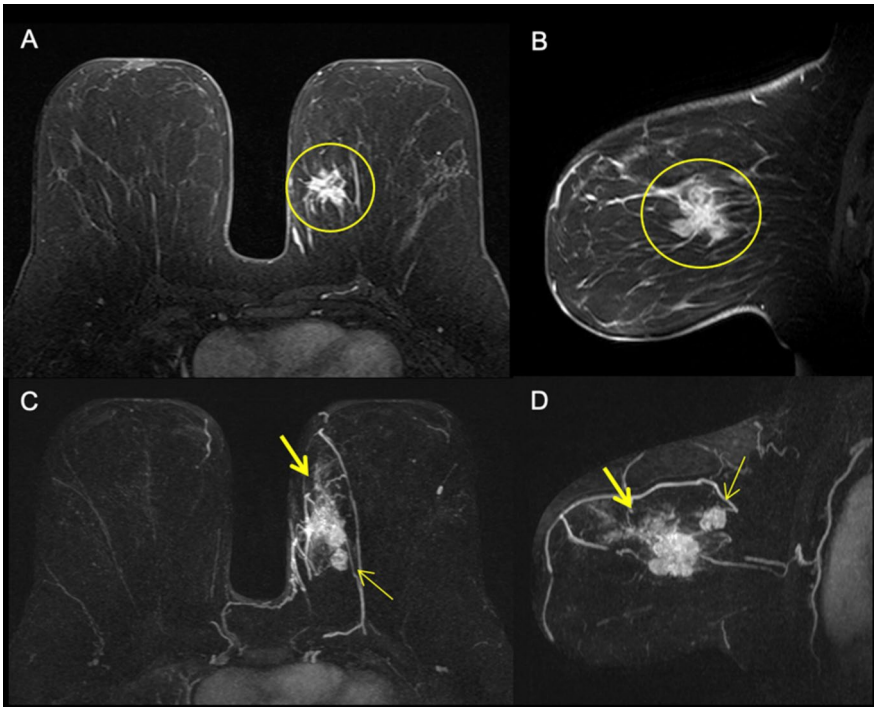

Figure 3. Irregular mass in the left breast (circle) with a satellite mass (thin arrow) and associated NME (thick arrow). IHC: Luminal B subtype (ER 95%, PgR 70%, HER2 -, Ki67 40%).

RNA sequencing, and less favourable prognosis, frequently warranting chemotherapy[9,28–30]. Additionally, ER-low positive luminal tumours present prognosis similar to triple-negative breast cancer, when treated in the same way, questioning whether they should be considered a separate entity[31]. The optimal ER threshold remains controversial worldwide, and some studies define TNBC based on a threshold < 10% ER expression[32,33]. A study that also used MCA analysis to assess MRI features in breast cancer patients demonstrated that the triple-negative

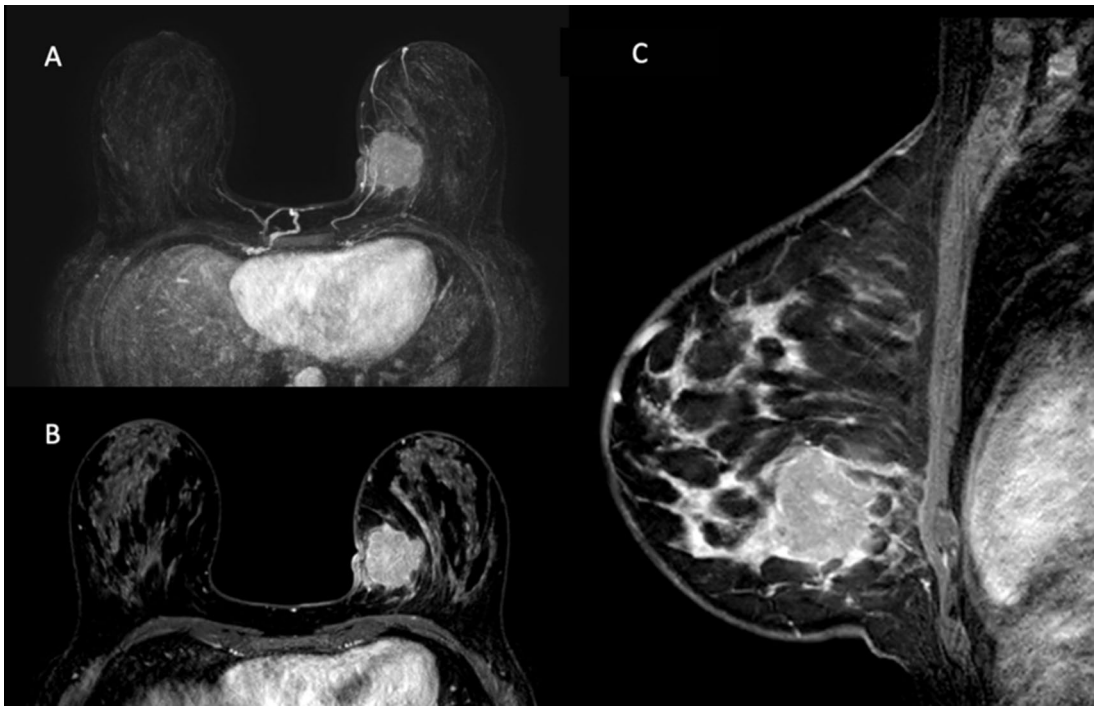

Figure 4. Round unifocal mass in the left breast. IHC: Luminal ER-low-positive (ER 5%, PgR -, HER2 -, Ki67 90%).

Variables	Luminal A	Luminal B	Luminal ER Low	HER2
Mass—shape				
Oval/round	0.31 (0.13–0.73) *p = 0.007*	0.42 (0.23–0.76) *p = 0.004*	0.95 (0.38–2.41) *p = 0.917*	0.32 (0.15–0.71) *p = 0.005*
Irregular	Ref	Ref	Ref	Ref
Mass—margins				
Circumscribed	0.24 (0.05–1.15) *p = 0.075*	0.11 (0.03–0.47) *p = 0.003*	0.50 (0.06–4.09) *p = 0.518*	0.21 (0.04–1.24) *p = 0.086*
Irregular	0.07 (0.02–0.23) *p < 0.001*	0.14 (0.05–0.37) *p < 0.001*	0.46 (0.11–1.88) *p = 0.278*	0.24 (0.08–0.73) *p = 0.012*
Spiculated	Ref	Ref	Ref	Ref
Mass—enhancement				
Homogeneous	32.00 (3.78–270.85) *p = 0.001*	8.50 (1.68–42.98) *p = 0.010*	2.29 (0.27–19.66) *p = 0.451*	5.33 (0.53–54.03) *p = 0.157*
Heterogeneous	5.82 (1.25–27.11) *p = 0.025*	2.98 (1.38–6.45) *p = 0.006*	0.83 (0.30–2.39) *p = 0.732*	5.70 (1.55–20.90) *p = 0.009*
Rim	Ref	Ref	Ref	Ref
Mass—late kinetic curve				
Persistent (type I)	14.04 (4.19–47.09) *p < 0.001*	2.47 (1.12–5.45) *p = 0.026*	1.56 (0.40–6.03) *p = 0.519*	1.40 (0.50–3.94) *p = 0.519*
Plateau (type II)	11.40 (3.55–36.66) *p < 0.001*	2.34 (1.14–4.82) *p = 0.021*	3.30 (1.14–9.54) *p = 0.028*	2.16 (0.90–5.17) *p = 0.084*
Washout (type III)	Ref	Ref	Ref	Ref
Lesion presentation	0.78			
Unifocal mass	(0.37–1.67) *p = 0.529* Ref	0.52 (0.29–0.92) *p = 0.026*	1.18 (0.44–3.11) *p = 0.744*	0.46 (0.23–0.93) *p = 0.031*
Multifocal mass/NME		Ref	Ref	Ref

Table 3. Multinomial regression analysis of MRI features associated with the immunophenotypes of NST invasive breast carcinomas, with the triple-negative phenotype as the reference.

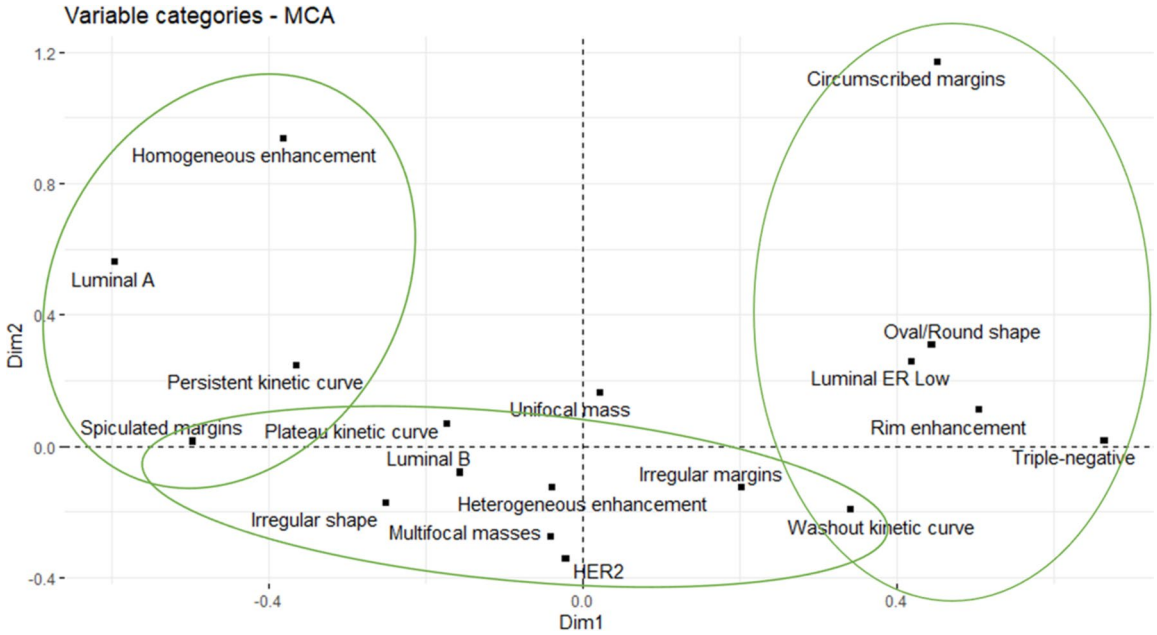

Figure 5. Multiple correspondence analysis (MCA) of MRI features and immunophenotypes of NST invasive breast carcinomas.

subtype, defined as ER < 10%, was associated with circumscribed margins, elevated TILs levels, a high KI-67 index and a complete pathological response following neoadjuvant chemotherapy[34].

The breast radiologist should be aware of imaging findings of different breast cancer subtypes for a proper radiopathology correlation. There is a great deal of concordance between IHC-assessed molecular subtypes on needle biopsy and surgical specimens; however, 10–20% of cases may show different results[35,36]. In contrast, imaging can provide whole-tumour assessment, so we suggest a three-group classification of MRI phenotypes to better correlate with the pathological features. The first group includes tumours presenting as a unifocal mass with spiculated margins and a persistent kinetic curve; this group is associated with slow-growing breast cancer, usually related to the luminal A immunophenotype. The second group includes tumours presenting as a mass with irregular shape and margins, heterogeneous internal enhancement and a plateau or washout kinetic curve, with or without the presence of NME, multifocal or multicentric disease; this imaging phenotype represents more aggressive tumours, usually with associated DCIS, which is most often associated with luminal B and HER2-overexpressed carcinomas. The third group includes tumours presenting as a mass with oval or round shape, circumscribed margins, rim enhancement, and a washout kinetic curve, which represents fast-growing carcinomas and was usually associated with triple-negative and luminal ER-low-positive subtypes in our sample. Cases with discordance between the imaging phenotype and the immunophenotype on needle biopsy should be discussed individually to assess the need for repeated IHC analysis after a new biopsy or surgical resection.

There were limitations associated with the present study. First, this retrospective study was conducted at a single cancer centre. Second, other imaging methods, such as ultrasonography and mammography, were not evaluated. Third, other MRI features previously correlated with breast cancer subtypes, such as diffusion-weighted imaging and T2 signal, were not assessed in this study. Because of the small number of patients with NME, the association between NME distribution and immunophenotypes were not included in the analysis.

Conclusion

In conclusion, our results demonstrate that MRI findings are closely related to the breast cancer immunophenotype, as described in previous studies. Additionally, we demonstrated that luminal ER-low-positive tumours present similar MRI findings to triple-negative tumours. This result must be confirmed in future studies, but it suggests that MRI can take on a fundamental role in adequate radiopathological correlation and therapeutic planning in these cases. Personalized treatment plans, tailored to the unique characteristics of the tumour and patient, are important for optimizing therapeutic outcomes and minimizing side effects. A multidisciplinary team approach, including radiologists, pathologists, oncologists and surgeons, is essential for the optimal management of patients with ER-low-positive breast cancer.

Data availability

The data supporting the results of this study are available upon request from the corresponding author. The data analyses and codes used to generate the results can also be made available upon request. In case of data requests, please contact Carla Chizuru Tajima via email at carlatajima@gmail.com.

Received: 5 May 2024; Accepted: 8 August 2024
Published online: 20 August 2024

References

1. Giuliano, A. E. *et al.* Breast cancer-major changes in the American Joint Committee on cancer eighth edition cancer staging manual. *CA Cancer J. Clin.* **67**, 290–303. https://doi.org/10.3322/caac.21393 (2017).
2. Kalli, S. *et al.* American joint committee on cancer's staging system for breast cancer, eighth edition: What the radiologist needs to know. *Radiographics* **38**, 1921–1933. https://doi.org/10.1148/rg.2018180056 (2018).
3. Allison, K. H. *et al.* Estrogen and progesterone receptor testing in breast cancer: ASCO/CAP guideline update. *J. Clin. Oncol.* **38**, 1346–1366. https://doi.org/10.1200/jco.19.02309 (2020).
4. Yi, M. *et al.* Which threshold for ER positivity? A retrospective study based on 9639 patients. *Ann. Oncol.* **25**, 1004–1011. https://doi.org/10.1093/annonc/mdu053 (2014).
5. Rajc, J., Fröhlich, I., Mrčela, M., Tomaš, I. & Flam, J. Prognostic impact of low estrogen and progesterone positivity in luminal B (Her2 negative) breast cancer. *Acta Clin. Croat.* **57**, 425–433. https://doi.org/10.20471/acc.2018.57.03.04 (2018).
6. Balic, M., Thomssen, C., Würstlein, R., Gnant, M. & Harbeck, N. St. Gallen/Vienna 2019: A brief summary of the consensus discussion on the optimal primary breast cancer treatment. *Breast Care (Basel)* **14**(2019), 103–110. https://doi.org/10.1159/000499931 (2019).
7. Kuerer, H. M. *et al.* Eliminating breast surgery for invasive breast cancer in exceptional responders to neoadjuvant systemic therapy: A multicentre, single-arm, phase 2 trial. *Lancet Oncol.* **23**, 1517–1524. https://doi.org/10.1016/s1470-2045(22)00613-1 (2022).
8. Yu, K. D., Cai, Y. W., Wu, S. Y., Shui, R. H. & Shao, Z. M. Estrogen receptor-low breast cancer: Biology chaos and treatment paradox. *Cancer Commun. (Lond.)* **41**, 968–980. https://doi.org/10.1002/cac2.12191 (2021).
9. Reinert, T. *et al.* Clinical implication of low estrogen receptor (ER-low) expression in breast cancer. *Front. Endocrinol. (Lausanne)* **13**, 1015388. https://doi.org/10.3389/fendo.2022.1015388 (2022).
10. Mann, R. M., Cho, N. & Moy, L. Breast MRI: State of the art. *Radiology* **292**, 520–536. https://doi.org/10.1148/radiol.2019182947 (2019).
11. Marino, M. A., Helbich, T., Baltzer, P. & Pinker-Domenig, K. Multiparametric MRI of the breast: A review. *J. Magn. Reson. Imaging* **47**, 301–315. https://doi.org/10.1002/jmri.25790 (2018).
12. Boisserie-Lacroix, M. *et al.* Correlation between imaging and molecular classification of breast cancers. *Diagn. Interv. Imaging* **94**, 1069–1080. https://doi.org/10.1016/j.diii.2013.04.010 (2013).
13. Net, J. M. *et al.* Relationships between human-extracted MRI tumor phenotypes of breast cancer and clinical prognostic indicators including receptor status and molecular subtype. *Curr. Probl. Diagn. Radiol.* **48**, 467–472. https://doi.org/10.1067/j.cpradiol.2018.08.003 (2019).
14. Vilar, L. N. *et al.* MR imaging findings in molecular subtypes of breast cancer according to BIRADS system. *Breast J.* **23**, 421–428. https://doi.org/10.1111/tbj.12756 (2017).
15. Grimm, L. J. *et al.* Relationships between MRI breast imaging-reporting and data system (BI-RADS) lexicon descriptors and breast cancer molecular subtypes: Internal enhancement is associated with luminal B subtype. *Breast J.* **23**, 579–582. https://doi.org/10.1111/tbj.12799 (2017).
16. Öztürk, V. S. *et al.* The relationship between MRI findings and molecular subtypes in women with breast cancer. *Curr. Probl. Diagn. Radiol.* **49**, 417–421. https://doi.org/10.1067/j.cpradiol.2019.07.003 (2020).
17. Ab Mumin, N., Hamid, M. T. R., Wong, J. H. D., Rahmat, K. & Ng, K. H. Magnetic resonance imaging phenotypes of breast cancer molecular subtypes: A systematic review. *Acad. Radiol.* **29**(Suppl 1), S89–S106. https://doi.org/10.1016/j.acra.2021.07.017 (2022).
18. Wolff, A. C. *et al.* Human epidermal growth factor receptor 2 testing in breast cancer: American society of clinical oncology/college of American pathologists clinical practice guideline focused update. *J. Clin. Oncol.* **36**, 2105–2122. https://doi.org/10.1200/jco.2018.77.8738 (2018).
19. Morris, E. A., Comstock, C. E. & Lee, C. H. ACR BI-RADS® magnetic resonance imaging. In *ACR BI-RADS® Atlas, Breast Imaging Reporting and Data System* (American College of Radiology, 2012).
20. Boisserie-Lacroix, M. *et al.* Radiological features of triple-negative breast cancers (73 cases). *Diagn. Interv. Imaging* **93**, 183–190. https://doi.org/10.1016/j.diii.2012.01.006 (2012).
21. Chen, J. H. *et al.* Triple-negative breast cancer: MRI features in 29 patients. *Ann. Oncol.* **18**, 2042–2043. https://doi.org/10.1093/annonc/mdm504 (2007).
22. Dogan, B. E., Gonzalez-Angulo, A. M., Gilcrease, M., Dryden, M. J. & Yang, W. T. Multimodality imaging of triple receptor-negative tumors with mammography, ultrasound, and MRI. *AJR Am. J. Roentgenol.* **194**, 1160–1166. https://doi.org/10.2214/ajr.09.2355 (2010).
23. Dogan, B. E. & Turnbull, L. W. Imaging of triple-negative breast cancer. *Ann. Oncol.* **23**(Suppl 6), 23–29. https://doi.org/10.1093/annonc/mds191 (2012).
24. Uematsu, T., Kasami, M. & Yuen, S. Triple-negative breast cancer: Correlation between MR imaging and pathologic findings. *Radiology* **250**, 638–647. https://doi.org/10.1148/radiol.2503081054 (2009).
25. Grimm, L. J., Johnson, K. S., Marcom, P. K., Baker, J. A. & Soo, M. S. Can breast cancer molecular subtype help to select patients for preoperative MR imaging?. *Radiology* **274**, 352–358. https://doi.org/10.1148/radiol.14140594 (2015).
26. Ha, R. *et al.* Breast cancer molecular subtype as a predictor of the utility of preoperative MRI. *AJR Am. J. Roentgenol.* **204**, 1354–1360. https://doi.org/10.2214/ajr.14.13666 (2015).
27. Gweon, H. M. *et al.* The clinical significance of accompanying NME on preoperative MR imaging in breast cancer patients. *PLoS ONE* **12**, e0178445. https://doi.org/10.1371/journal.pone.0178445 (2017).
28. Curigliano, G. *et al.* St Gallen consensus conference panelists 2023, understanding breast cancer complexity to improve patient outcomes: The St Gallen international consensus conference for the primary therapy of individuals with early breast cancer 2023. *Ann. Oncol.* **34**, 970–986. https://doi.org/10.1016/j.annonc.2023.08.017 (2023).
29. Iwamoto, T. *et al.* Estrogen receptor (ER) mRNA and ER-related gene expression in breast cancers that are 1% to 10% ER-positive by immunohistochemistry. *J. Clin. Oncol.* **30**, 729–734. https://doi.org/10.1200/JCO.2011.36.2574 (2012).
30. Villegas, S. L. *et al.* Therapy response and prognosis of patients with early breast cancer with low positivity for hormone receptors: An analysis of 2765 patients from neoadjuvant clinical trials. *Eur. J. Cancer* **148**, 159–170. https://doi.org/10.1016/j.ejca.2021.02.020 (2021).
31. Acs, B. *et al.* Real-world overall survival and characteristics of patients with ER-zero and ER-low HER2-negative breast cancer treated as triple-negative breast cancer: A Swedish population-based cohort study. *Lancet Reg. Health Eur.* **40**, 100886. https://doi.org/10.1016/j.lanepe.2024.100886 (2024).
32. Johnson, H. M. *et al.* Patient-reported outcomes of omission of breast surgery following neoadjuvant systemic therapy: A nonrandomized clinical trial. *JAMA Netw. Open* **6**, e2333933. https://doi.org/10.1001/jamanetworkopen.2023.33933 (2023).
33. Dieci, M. V. *et al.* Impact of estrogen receptor levels on outcome in non-metastatic triple negative breast cancer patients treated with neoadjuvant/adjuvant chemotherapy. *NPJ Breast Cancer* **7**, 101. https://doi.org/10.1038/s41523-021-00308-7 (2021).
34. Malhaire, C. *et al.* Exploring the added value of pretherapeutic MR descriptors in predicting breast cancer pathologic complete response to neoadjuvant chemotherapy. *Eur. Radiol.* **33**, 8142–8154. https://doi.org/10.1007/s00330-023-09797-5 (2023).

35. Pölcher, M. *et al.* Concordance of the molecular subtype classification between core needle biopsy and surgical specimen in primary breast cancer. *Arch. Gynecol. Obstet.* **304**, 783–790. https://doi.org/10.1007/s00404-021-05996-x (2021).
36. You, K. *et al.* Comparison of core needle biopsy and surgical specimens in determining intrinsic biological subtypes of breast cancer with immunohistochemistry. *J. Breast Cancer* **20**, 297–303. https://doi.org/10.4048/jbc.2017.20.3.297 (2017).

Author contributions

F.P.S.G.A., V.C.M., and J.M.F. conducted data collection. B.B. B.performed statistical analysis. C.C.T. wrote the manuscript and prepared figures and tables/graphs. C.A.B.T.O., M.S., and A.G.V.B. conducted manuscript review.

Competing interests

The authors declare no competing interests.

Additional information

Correspondence and requests for materials should be addressed to C.C.T.

Reprints and permissions information is available at www.nature.com/reprints.

Publisher's note Springer Nature remains neutral with regard to jurisdictional claims in published maps and institutional affiliations.